Virus Research 304 (2021) 198524

Contents lists available at ScienceDirect

Virus Research

journal homepage: www.elsevier.com/locate/virusres

A study of the effects of age on the dynamics of RSV in animal models

Shaheer Khan, Hana M. Dobrovolny *

Department of Physics and Astronomy, Texas Christian University, Fort Worth, TX USA

ARTICLE INFO

Keywords:
Respiratory syncytial virus
Pediatric
Immune development
Mathematical model
Parameter estimation

ABSTRACT

Respiratory syncytial virus can cause severe illness and even death, particularly in infants. The increased severity of disease in young children is thought to be due to a lack of previous exposure to the virus as well as the limited immune response in infants. While studies have examined the clinical differences in disease between infants and adults, there has been limited examination of how the viral dynamics differ as infants develop. In this study, we apply a mathematical model to data from cotton rats and ferrets of different ages to assess how viral kinetics parameters change as the animals age. We find no clear trend in the viral decay rate, infecting time, and basic reproduction number as the animals age. We discuss possible reasons for the null result including the limited data, lack of detail of the mathematical model, and the limitations of animal models.

1. Introduction

Respiratory syncytial virus (RSV) causes an acute respiratory illness that can be particularly severe in infants and young children (Anderson et al., 2016; Borchers et al., 2013; Stein et al., 2017). Clinically, young children experience higher mortality and hospitalization rates (Anderson et al., 2016; Borchers et al., 2013; Stein et al., 2017). They experience more severe symptoms and are more likely to have infections spread to the lower respiratory tract (Kabego et al., 2018; Shi et al., 2015; Ueno et al., 2019; Zar et al., 2020). They are also more likely to have long-lasting health consequences such as wheezing and asthma (Backman et al., 2014; Baraldi et al., 2020; Coutts et al., 2020; Fauroux et al., 2017) after infection with RSV. Healthy adults, on the other hand, experience only mild illness (Bagga et al., 2013; Hall et al., 2001; Lee et al., 2004; Mills et al., 1971). An understanding of how the dynamics of the infection change as humans age can help us develop better treatment strategies for the vulnerable infant population.

Some of the change in RSV infection dynamics between children and adults is thought to be due to differences in the immune response (Chung et al., 2007; Drajac et al., 2017; Lambert et al., 2014; Mcintosh et al., 1978). Until about 6 months of age, infants are protected by maternal antibodies (Chu et al., 2014; Walsh et al., 2018) and the innate immune response (Piedra et al., 2017). There is even some evidence that in early childhood some cells actively suppress the immune response (Elahi et al., 2013). At about 4 months of age, the adaptive immune response starts to develop (Sande et al., 2014; Trento et al., 2017). This developing immune system results in markedly different immune responses to RSV in children and infants as compared to healthy adults. Studies have shown that there is a delay in the pulmonary cytokine response (Boukhvalova et al., 2007), an attenuated IFN I response (Marr et al., 2014), and an imbalance of chemokines (Boukhvalova et al., 2007; Eichinger et al., 2017; Shrestha et al., 2017) in young children as compared to adults. Cytotoxic T cells are also known to be functionally different in children than in adults (Mold et al., 2010). While some details of the pediatric immune response are known, teasing out their effect on the viral time course of RSV is difficult.

One technique for quantifying the basic biological processes underlying the viral time course is mathematical modeling. Mathematical models of the in-host dynamics of viral infections have been used to quantitatively describe the infection process for many different viral infections (Baccam et al., 2006; González-Parra et al., 2018; Hernandez-Vargas and Velasco-Hernandez, 2020; Liao et al., 2020), including RSV (Beauchemin et al., 2019; González-Parra et al., 2018a; González-Parra and Dobrovolny, 2015; 2018b; Wethington et al., 2019). The ability of mathematical models to quantify the timescale of infection processes has been exploited to quantitatively compare infections caused by different strains of virus (Paradis et al., 2015; Petrie et al., 2015; Pinilla et al., 2012; Simon et al., 2016), infections caused by different viruses (González-Parra et al., 2018a), or infections in different systems (González-Parra and Dobrovolny, 2018b). These types of studies have pinpointed which steps in the viral replication cycle differ between the infections being compared, and have quantified the change. This type of study was recently performed using some of the data used in this study (Wethington et al., 2019), finding age-dependent differences in

* Corresponding author.
E-mail address: h.dobrovolny@tcu.edu (H.M. Dobrovolny).

https://doi.org/10.1016/j.virusres.2021.198524
Received 27 January 2021; Received in revised form 24 June 2021; Accepted 17 July 2021
Available online 28 July 2021

the initial viral concentration, the ratio of decay time to production time, and the onset of the immune response.

Building on this effort, we use a viral kinetics model to quantitatively compare RSV infections in young and adult animals. We use the data from studies of cotton rats (Prince et al., 1978) that was used in the Wethington et al. study (Wethington et al., 2019), but include measurements from all three regions of the respiratory tract (nose, trachea, and lung). We also include analysis of data from a second experiment using ferrets (Prince and Porter, 1976) of different ages to estimate the parameters of a mathematical model of RSV infection and determine if they change as the animals age.

2. Material and methods

2.1. Viral kinetics model

We use a simple model describing the viral replication cycle first used to describe influenza (Baccam et al., 2006), but more recently also used to describe respiratory syncytial virus dynamics in African green monkeys (González-Parra and Dobrovolny, 2018a).

$$\begin{aligned} \dot{T} &= -\beta TV \\ \dot{E} &= \beta TV - kE \\ \dot{I} &= kE - \delta I \\ \dot{V} &= pI - cV \end{aligned} \tag{1}$$

In this model, uninfected target cells, T, are infected by the virions, V, at rate β. The infected cells transition into an eclipse phase, E, where they are not yet producing virus. The eclipse cells transition to infectious cells, I, at rate k with infectious cells dying at rate δ. Virus is actively produced by the infectious cells at rate p and virus is cleared at rate c.

Since some of the parameters depend on units of virus, which are not standardized and thus not easily compared from one experiment to another, we use the parameter estimates to derive quantities that more readily quantify different processes during the course of the infection. The viral decay rate is the minimum of c, k, and δ (Smith et al., 2010) and gives a measure of how quickly virus is being eliminated once there are few target cells remaining. The basic reproduction number ($R_0 = \beta p T_0 / c\delta$), where T_0 is the initial number of target cells, is the number of secondary infections resulting from a single infected cell and gives a measure of the ease or difficulty of virus spread between cells. The infecting time ($t_{inf} = \sqrt{2/p\beta T_0}$) is the time between the release of a virion from one cell and infection of the next cell. Note that this model does not include an explicit immune response, but changes in the infection caused by the immune response can be captured by changes in the parameter values (González-Parra and Dobrovolny, 2018b). For example, we expect the viral decay rate to be higher in animals where the antibody response has developed and is helping to clear virus from the respiratory tract.

2.2. Experimental data

Viral titers were obtained from two previous studies (Prince et al., 1978; Prince and Porter, 1976) that examined aging in cotton rats and ferrets. In the first data set, cotton rats (*Sigmodon hispidus*) of ages 3, 14, 28, or 40 days were infected intranasally with 10^4 pfu of long strain RSV. Virus titer was measured over a period of 20 days in the lungs, trachea, and nose. 3 animals were sacrificed at each time point, so the data does not represent the viral time course for an individual animal, but is the geometric mean of viral load measured in different sets of animals at each time point. Since the raw experimental data after day 9 usually fell below the level of detection, the compiled data sets do not extend beyond day 9.

In the second data set, ferrets of ages 0, 3, 7, 14, or 28 days were infected intranasally with 3.6×10^3 pfu of the long strain of RSV. Virus was measured from lung and nasal tissue homogenates daily until 10 days post-infection (dpi). Two separate litters of ferrets were used and data was presented separately for each group. At each time point, one animal from each of the litters was sacrificed, so this data also does not represent the viral time course in an individual animal. Data was extracted from figures in both papers using WebPlotDigitizer (https://automeris.io/WebPlotDigitizer/).

2.3. Fitting algorithms

To determine the best fit, the sum of squared residuals (SSR) between the experimental and predicted values was minimized. The SSR is calculated as

$$\mathrm{SSR} = \sum_{i=1}^{n} \left(\log_{10}(y_i) - \log_{10}(f(t_i))\right)^2, \tag{2}$$

where n is the number of experimental data points, y_i are the experimentally measured viral loads, and $f(t_i)$ are the model predictions of viral load (V) at time t_i. All data points are weighted equally. To fit the model to the experimental data, the viral kinetic model was solved using Python's `odeint` function. The SSR was minimized using the Nelder Mead algorithm of Python's `minimize` function. We assumed that infections were started with an initial viral inoculum (determined through fitting) and we set the initial number of target cells to 1 ($T_0 = 1$, i.e. we measured cells relative to the initial number present). We assumed that there are initially no eclipse or infectious cells ($E_0 = I_0 = 0$).

We used the Monte Carlo Markov Chain (MCMC) technique to estimate the 95% confidence intervals of our best fit parameters. This was implemented using python's emcee package using 50 walkers initialized in a hypersphere about the best fit estimate. The assumed prior distributions for each parameter were uniform distributions encompassing a broad range of possible values: (10^{-8}–10^{-2}g·(pfu·d)$^{-1}$) for β, (10^4–10^{10}pfu·(g·d)$^{-1}$) for p, (10^{-3}–100/d) for c, k, and δ, and (10^{-3}–10^5pfu/g) for V_0. The algorithm was run for 1000 steps after a burn-in of 100 steps.

3. Results

3.1. Aging in cotton rats

Fits of the viral kinetics model to RSV infection in cotton rats are shown in Fig. 1 with associated parameter values given in Table 1. Correlation and parameter distribution plots are included in the supplementary material. Note that we have fit the viral kinetics model separately to the viral titer measurements in the lung (left column), trachea (center column), and nose (right column). Some of these parameters have been estimated for RSV in vitro (Beauchemin et al., 2019; González-Parra et al., 2018a; González-Parra and Dobrovolny, 2018b), in other animals (González-Parra and Dobrovolny, 2018a; 2018b), and in humans (González-Parra and Dobrovolny, 2015; 2018b). Our estimates for the infecting time are lower than estimates of in vitro infections (Beauchemin et al., 2019), but in line with estimated infecting times for in vivo infections (González-Parra and Dobrovolny, 2015; 2018b). The basic reproduction number found here is also in line with previous estimates for RSV infections (Beauchemin et al., 2019; González-Parra and Dobrovolny, 2018a).

For easier interpretation of any changes in parameter values as the rats age, we plot the posterior distributions determined from MCMC for viral decay rate, basic reproduction number, and infecting time as functions of age in Fig. 2. We see no clear trend in any of the parameters as the rats age. The distributions for all three parameters overlap for all ages, indicating that there is no statistically discernible age-dependent difference in parameters. There are some slight changes in the parameter distributions when comparing distributions for nose, trachea, and lungs. The distribution for the decay rate in the lungs has a larger tail on the right as compared to the distributions for nose and trachea.

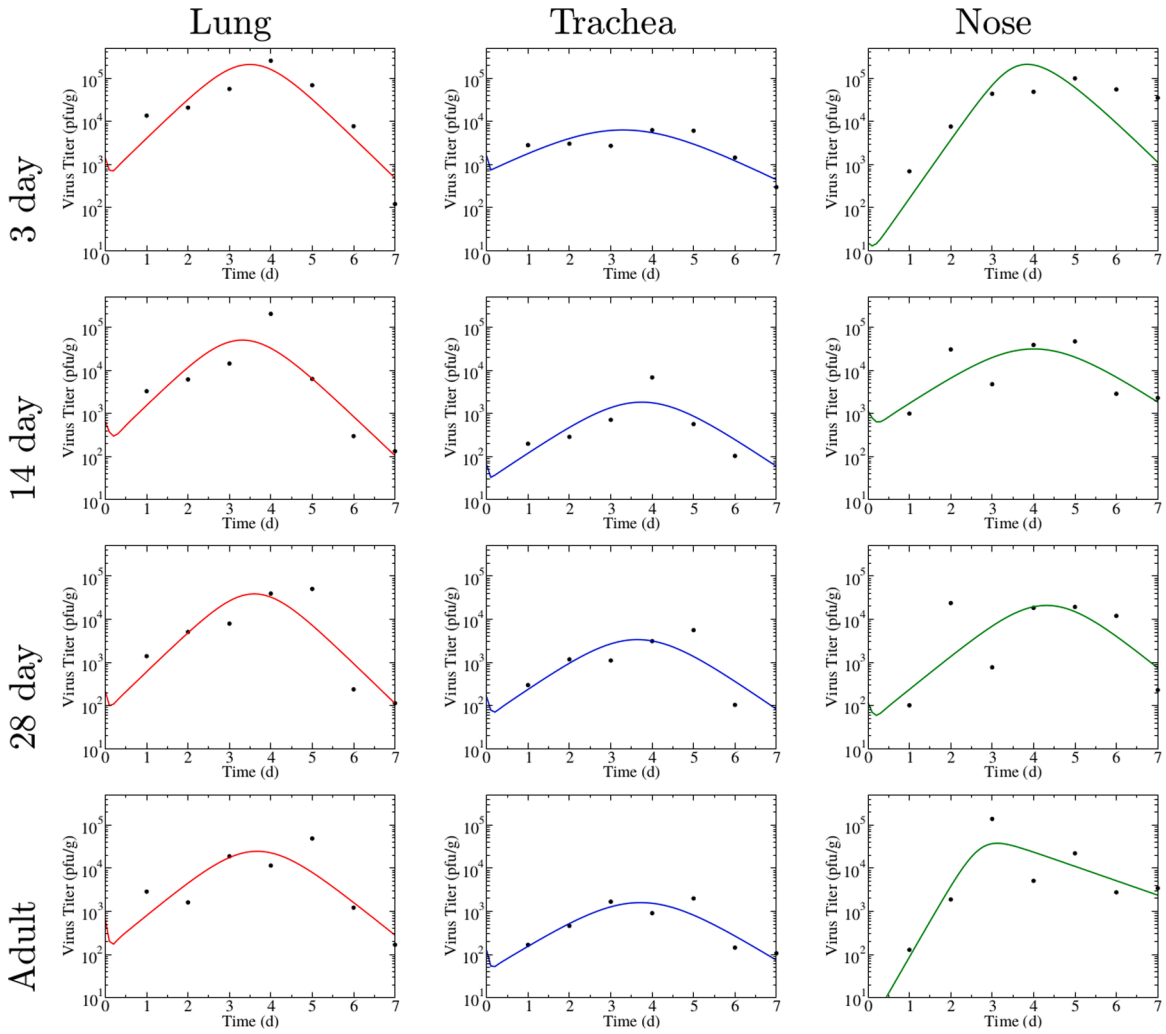

Fig. 1. Experimental data (black dots) is plotted with the viral model predictions (solid lines). Data represents RSV infections in different aged (rows) cotton rats with viral titer measurements taken from the lung (left column), trachea (center column), and nose (right column).

Similarly, the distribution for R_0 in the nose has the longest tail on the right while the distribution for $t_i nf$ in the trachea has the longest tail.

3.2. Aging in ferrets

We performed a similar analysis using data taken from aging ferrets. In this case, the viral load measurements are taken from nasal tissues only, but from two different litters of ferrets. Model fits to the experimental data are shown in Fig. 3 with corresponding parameters given in Table 2. Correlation plots and parameter distributions for the estimated parameters are included in the supplemental materials. In many of the fits to the ferret data, we see a correlation between the parameters β and p, but no clear correlation between other parameters. Infecting times are similar to those found in the cotton rats, although the basic reproduction number is somewhat higher in some cases.

Again, we plot the posterior distributions of viral decay rate, infecting time, and basic reproduction numbers for different ages of ferrets (Fig. 4). While it is possible to more clearly differentiate some of the distributions by eye for the ferrets than it is for the cotton rats, there is still substantial overlap of the distributions, indicating no significant difference in the parameters as the ferrets age.

4. Discussion

This study used mathematical models to quantify the effect of aging on several parameters that characterize RSV infection. Specifically, we compared the viral decay rate, basic reproduction number, and infecting time by fitting a mathematical model to viral titer measurements from RSV infections. We did not find a clear trend in any of those three parameters as a function of the age of the animal in either cotton rats or ferrets. While we did not find a trend in the parameters we examined, a recent study of age-related differences in RSV infections in cotton rats noted an increased viral titer peak and lower levels of interferon in young rats (Wen et al., 2019) as compared to adult rats. Unfortunately, this study used only three cohorts of rats (young, adult, elderly), making it difficult to clearly identify age-related trends.

Our study involves young animals whose immune response is developing, so we might expect that parameters reflecting the influence of the immune response would change systematically with age. In this study, the immune response is primarily reflected in the viral decay rate, which is affected by the presence of antibodies and the presence of cytotoxic T lymphocytes (CTLs). As the immune response increases, we expect the viral decay rate to increase — when antibodies (or CTLs) are present, virus (or infectious cells) are cleared from the body faster and will therefore lead to more rapid clearance of the virus (Cao et al., 2016; Dobrovolny et al., 2013). We do not observe such a clear trend. There are also reports of more severe infections with higher viral loads in pediatric patients (Anderson et al., 2016; Borchers et al., 2013; Stein et al., 2017; Uusitupa et al., 2020; Zhou et al., 2015). Higher viral loads will be reflected in the basic reproductive number, so we expect that this

Table 1
Best fit parameter estimates for cotton rats of different ages.

Parameter	3 days	14 days	28 days	40 days	Prior
		Lungs			
β (g·(pfu·d)$^{-1}$)	3.90×10^{-7}	2.78×10^{-6}	1.62×10^{-6}	2.54×10^{-6}	10^{-8}–10^{-2}
95% CI	$(0.371–69100) \times 10^{-7}$	$(0.718–4230) \times 10^{-6}$	$(0.0373–8380) \times 10^{-6}$	$(0.0147–7540) \times 10^{-6}$	
k (/d)	8.48	4.24	10.94	6.03	10^{-3}–10^{2}
95% CI	0.0302–84.9	0.00277–81.4	0.00158–80.7	0.00152–80.4	
δ (/d)	8.48	4.73	10.94	6.62	10^{-3}–10^{2}
95% CI	0.0132–84.8	0.0546–90.2	0.0191–91.0	0.00282–78.2	
p (pfu·(g·d)$^{-1}$)	3.53×10^{8}	3.11×10^{7}	1.26×10^{8}	6.86×10^{7}	10^{4}–10^{10}
95% CI	$(0.000338–69.7) \times 10^{8}$	$(0.00227–249) \times 10^{7}$	$(0.000163–13.1) \times 10^{8}$	$(0.00124–269) \times 10^{7}$	
c (/d)	8.49	6.22	10.92	14.09	10^{-3}–10^{2}
95% CI	0.00293–79.1	0.00427–76.1	0.00350–72.7	0.00157–84.1	
V_0 (pfu/g)	1.44×10^{4}	6.50×10^{3}	2.16×10^{3}	6.50×10^{3}	10^{-3}–10^{5}
95% CI	$0.0132–9.21 \times 10^{4}$	$0.00423–7.82 \times 10^{4}$	$0.00438–8.67 \times 10^{4}$	$0.0101–8.76 \times 10^{4}$	
R_0	1.90	3.27	1.70	2.05	
95% CI	6.90×10^{-3}–3.59×10^{4}	$0.919–2.57 \times 10^{4}$	$0.0416–6.27 \times 10^{4}$	$0.121–1.65 \times 10^{5}$	
t_{inf} (h)	2.85	3.66	2.38	2.57	
95% CI	0.732–102	0.0298–72.7	0.0461–454	0.0414–487	
		Trachea			
β (g·(pfu·d)$^{-1}$)	1.19×10^{-6}	1.10×10^{-5}	1.17×10^{-5}	1.55×10^{-5}	10^{-8}–10^{-2}
95% CI	$(0.0121–6550) \times 10^{-6}$	$(0.00126–748) \times 10^{-5}$	$(0.00128–763) \times 10^{-5}$	$(0.00147–769) \times 10^{-5}$	
k (/d)	17.9	15.1	8.80	10.9	10^{-3}–10^{2}
95% CI	0.00137–81.2	0.00140–71.6	0.00141–77.6	0.00135–77.3	
δ (/d)	54.6	26.8	8.81	11.3	10^{-3}–10^{2}
95% CI	0.00240–90.4	0.00271–85.5	0.00242–83.1	0.00203–79.7	
p (pfu·(g·d)$^{-1}$)	9.61×10^{8}	3.94×10^{7}	1.07×10^{7}	1.15×10^{7}	10^{4}–10^{10}
95% CI	$(0.000119–27.6) \times 10^{8}$	$(0.00123–46.5) \times 10^{7}$	$(0.00113–46.0) \times 10^{7}$	$(0.00118–18.4) \times 10^{7}$	
c (/d)	18.4	12.5	8.84	11.3	10^{-3}–10^{2}
95% CI	0.00130–59.4	0.00130–71.1	0.00143–61.1	0.00131–67.5	
V_0 (pfu/g)	1.60×10^{4}	6.52×10^{2}	1.60×10^{3}	1.25×10^{3}	10^{-3}–10^{5}
95% CI	$5.33–9.06 \times 10^{4}$	$3.74–6.67 \times 10^{4}$	$4.76–8.14 \times 10^{4}$	$0.0387–7.31 \times 10^{4}$	
R_0	1.13	1.30	1.60	1.40	
95% CI	$0.00936–2.60 \times 10^{4}$	$0.00578–3.78 \times 10^{4}$	$0.00737–4.84 \times 10^{4}$	$0.0162–7.56 \times 10^{4}$	
t_{inf} (h)	1.00	1.63	3.04	2.55	
95% CI	0.149–854	0.150–1030	0.118–1240	0.131–910	
		Nose			
β (g·(pfu·d)$^{-1}$)	1.46×10^{-6}	2.14×10^{-6}	3.76×10^{-6}	1.16×10^{-5}	10^{-8}–10^{-2}
95% CI	$(0.532–5400) \times 10^{-6}$	$(0.0188–8230) \times 10^{-6}$	$(0.0227–7620) \times 10^{-6}$	$(0.00315–756) \times 10^{-5}$	
k (/d)	2.71	5.17	6.17	22.4	10^{-3}–10^{2}
95% CI	0.00194–68.9	0.00161–82.2	0.00199–68.6	0.00194–78.6	
δ (/d)	34.0	4.62	6.12	10.0	10^{-3}–10^{2}
95% CI	0.00330–83.9	0.00188–82.5	0.00170–80.4	0.00157–82.7	
p (pfu·(g·d)$^{-1}$)	3.18×10^{8}	2.03×10^{7}	2.11×10^{7}	6.46×10^{6}	10^{4}–10^{10}
95% CI	$(0.000728–35.1) \times 10^{8}$	$(0.00178–395) \times 10^{7}$	$(0.00155–131) \times 10^{7}$	$(0.0202–1140) \times 10^{6}$	
c (/d)	2.65	4.20	6.12	10.0	10^{-3}–10^{2}
95% CI	0.00197–59.3	0.00164–85.8	0.00165–78.0	0.00130–43.7	
V_0 (pfu/g)	1.53×10^{2}	1.16×10^{4}	1.18×10^{3}	2.81×10^{1}	10^{-3}–10^{5}
95% CI	$0.00203–4.72 \times 10^{4}$	$0.00366–9.18 \times 10^{4}$	$0.0108–7.64 \times 10^{4}$	$0.00311–6.92 \times 10^{4}$	
R_0	5.16	2.24	2.17	9.71	
95% CI	$4.05–1.90 \times 10^{6}$	$0.111–1.08 \times 10^{6}$	$0.151–3.66 \times 10^{5}$	$1.10–6.17 \times 10^{6}$	
t_{inf} (h)	1.57	5.15	3.80	3.92	
95% CI	0.0392–12.8	0.0134–337	0.0927–407	0.0576–186	

parameter should decrease with age, but we do not observe this trend in our study either. There is, however, contradictory evidence on this point, with other recent studies showing increased severity with lower viral loads in infants (Brenes-Chacon et al., 2021; Garcia-Maurino et al., 2019), so the expected trend in basic reproduction number with age is not clear-cut.

There are several possible reasons for the null findings of this study. It could be that the particular parameters we examined here do not change significantly with age, but that other parameters might show a clearer age-based trend. For example, a study using human RSV infection data found lower eclipse phase duration ($1/k$) and lower infectious lifespan ($1/\delta$) in pediatric patients as compared to healthy adults (González-Parra and Dobrovolny, 2018b). Another study that analyzed the cotton rat data used here found an abrupt change in the ratio of decay time to production time, denoted by τ_{ratio}, between the ages of 14 days and 28 days in the lung data (Wethington et al., 2019). The calculation of τ_{ratio} is based on linear fits to the rise and fall of viral load, so there is less of an issue with parameter identifiability. Wethington et al. also fit a mechanistic model that included a crude adaptive immune response to the lung data of cotton rats, finding that the initial

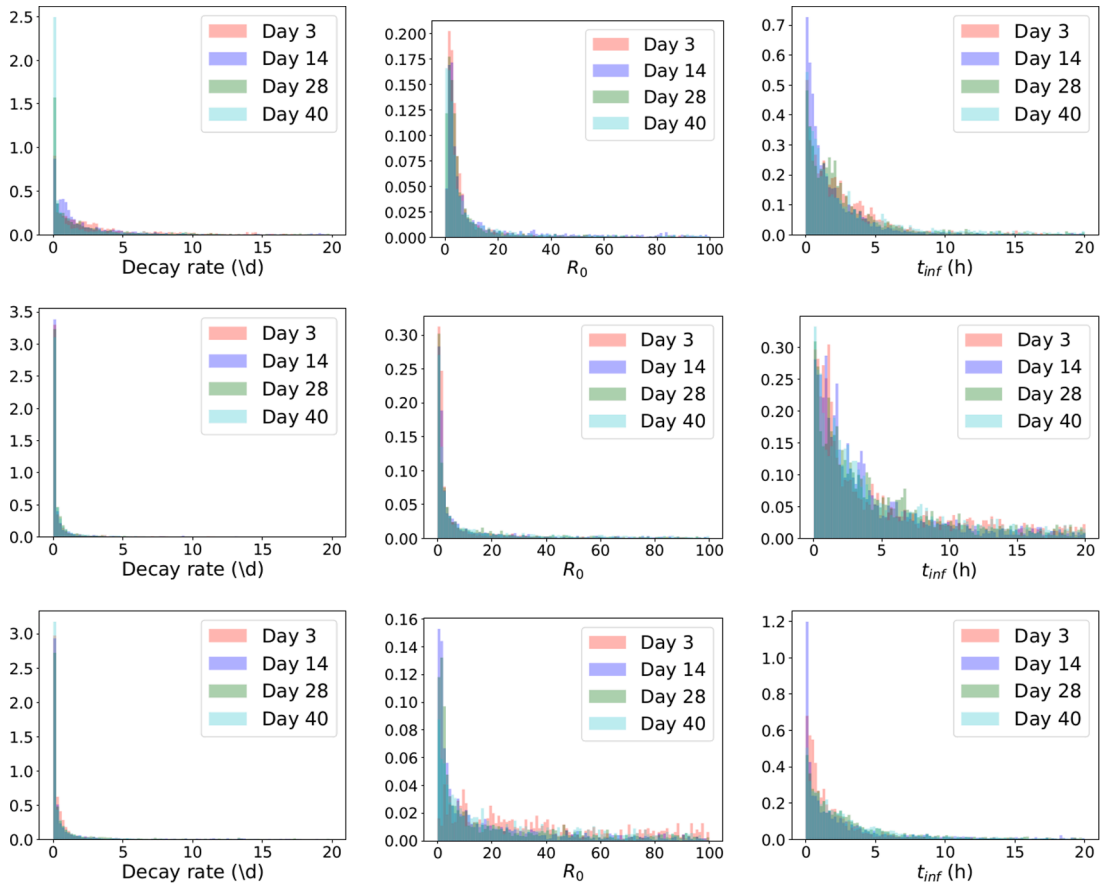

Fig. 2. Viral kinetics parameter estimates in different aged cotton rats. We show distributions for the viral decay rate (left column), basic reproduction number (center column), and infecting time (right column) in the lung (top row), trachea (center row), and nose (bottom row) for RSV infections in animals of different ages.

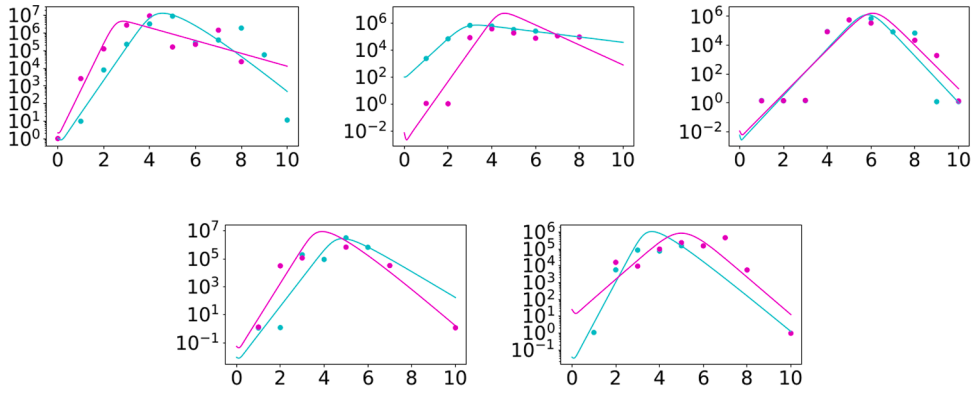

Fig. 3. Experimental data (dots) is plotted with the viral model predictions (solid lines) for ferret litter 1 (cyan) and ferret litter 2 (magenta). Data represents RSV infections in different aged ferrets at ages 0 (top left), 3d (top center), 7d (top right), 14d (bottom left), 28d (bottom right). (For interpretation of the references to color in this figure legend, the reader is referred to the web version of this article.)

viral inoculum decreased with age and the time at which the immune response started increased slightly with age. The authors attributed the decrease in viral inoculum to the expanding size of the lung. The correlation of onset of immune response with age was not strong and the magnitude of the change was less than a day. Although they used a different fitting methodology (nonlinear mixed effects modeling), they also found no significant age-dependence in the remaining parameters of their model.

In humans, there is also the confounding effect of previous infection, since 100% of people have had the infection by age two (Toivonen et al., 2020). Previous exposure to RSV results in an immune response that is primed to fight RSV re-infection (Blunck et al. (2021)), although the presence of antibodies wanes over time allowing for re-infection (Varga and Braciale, 2013). There is also evidence that RSV does not produce a robust T-cell response (Vojvoda et al., 2014), which might also contribute to its ability to reinfect with attenuated severity over a person's lifetime. Since the animals in these studies were housed in labs where exposure to infection could be controlled, they were presumably all immunologically naive to RSV. This means that any changes in dynamics observed in these studies are due only to age-related changes in immune response, whereas in humans RSV infection dynamics in anyone older than two are also mediated by a pre-existing adaptive

Table 2
Best fit parameter estimates for ferrets of different ages.

Parameter	0 days	3 days	7 days	14 days	28 days	Prior
			Ferret 1			
β (g·(pfu·d)$^{-1}$)	8.47×10^{-7}	5.42×10^{-6}	1.06×10^{-6}	3.52×10^{-6}	1.21×10^{-5}	10^{-8}–10^{-2}
95% CI	$(0.728–137) \times 10^{-7}$	$(0.0253–8220) \times 10^{-6}$	$(0.0194–14.8) \times 10^{-6}$	$(0.561–1140) \times 10^{-6}$	$(0.182–723) \times 10^{-5}$	
k (/d)	2.68	30.6	15.3	3.15	7.63	10^{-3}–10^{2}
95% CI	1.22–31.7	0.00199–91.9	4.01–73.9	0.00220–64.2	0.00347–74.6	
δ (/d)	2.68	12.1	15.1	5.98	2.83	10^{-3}–10^{2}
95% CI	1.15–62.5	0.00144–79.2	4.19–79.2	0.00327–60.4	0.00161–31.7	
p (pfu·(g·d)$^{-1}$)	1.52×10^{8}	1.25×10^{7}	4.16×10^{8}	5.11×10^{7}	9.86×10^{6}	10^{4}–10^{10}
95% CI	$(0.144–58.4) \times 10^{8}$	$(0.00544–208) \times 10^{7}$	$(0.107–51.8) \times 10^{8}$	$(0.0211–296) \times 10^{7}$	$(0.0455–1950) \times 10^{6}$	
c (/d)	2.68	0.46	15.1	2.15	2.49	10^{-3}–10^{2}
95% CI	1.19–70.0	0.00135–25.2	3.62–63.5	0.00134–37.3	0.00169–75.9	
V_0 (pfu/g)	1.10	1.01×10^{2}	5.79×10^{-3}	9.34×10^{-3}	3.68×10^{-2}	10^{-3}–10^{5}
95% CI	0.00405–101	$0.00286–5.57 \times 10^{4}$	0.00118–0.0975	0.00112–0.717	0.00117–19.1	
R_0	17.9	12.2	1.93	14.0	16.9	
95% CI	3.44–71.6	$3.48–6.26 \times 10^{7}$	1.43–4.66	$8.86–3.71 \times 10^{7}$	$9.98–1.71 \times 10^{7}$	
t_{inf} (h)	2.99	4.13	1.61	2.53	3.11	
95% CI	0.748–4.63	0.0553–20.3	0.698–3.42	0.107–6.25	0.0648–5.89	
			Ferret 2			
β (g·(pfu·d)$^{-1}$)	2.17×10^{-6}	1.40×10^{-6}	1.41×10^{-6}	1.71×10^{-6}	2.15×10^{-6}	10^{-8}–10^{-2}
95% CI	$(0.414–853) \times 10^{-6}$	$(7.27–3260) \times 10^{-6}$	$(0.330–34.0) \times 10^{-6}$	$(0.0947–131) \times 10^{-6}$	$(0.275–20.0) \times 10^{-6}$	
k (/d)	17.3	7.48	8.49	6.05	5.39	10^{-3}–10^{2}
95% CI	0.0313–84.8	0.00516–73.3	2.31–81.6	1.46–71.9	2.00–76.8	
δ (/d)	10.0	1.70	7.70	2.95	5.39	10^{-3}–10^{2}
95% CI	0.0430–87.1	0.00158–11.4	2.34–58.1	1.56–57.1	1.75–62.8	
p (pfu·(g·d)$^{-1}$)	7.02×10^{7}	1.86×10^{8}	1.32×10^{8}	8.60×10^{7}	4.40×10^{7}	10^{4}–10^{10}
95% CI	$(0.0405–113) \times 10^{7}$	$(0.000489–2.65) \times 10^{8}$	$(0.0298–24.1) \times 10^{8}$	$(0.301–588) \times 10^{7}$	$(0.237–298) \times 10^{7}$	
c (/d)	0.84	16.8	8.22	3.06	5.40	10^{-3}–10^{2}
95% CI	0.00169–7.74	0.00463–86.7	2.62–57.1	1.68–73.6	1.90–84.2	
V_0 (pfu/g)	2.19	7.67×10^{-3}	1.13×10^{-2}	5.27×10^{-2}	2.66×10^{1}	10^{-3}–10^{5}
95% CI	0.00135–4.03	0.00115–1.15	0.00131–0.299	0.00126–22.0	0.195–2110	
R_0	18.2	9.11	2.94	16.32	3.26	
95% CI	$6.79–7.91 \times 10^{5}$	$11.5–5.69 \times 10^{5}$	1.69–9.18	2.80–80.6	1.47–9.43	
t_{inf} (h)	2.75	2.10	2.49	2.80	3.49	
95% CI	0.200–5.52	0.121–6.67	0.814–4.43	0.547–4.05	0.874–6.45	

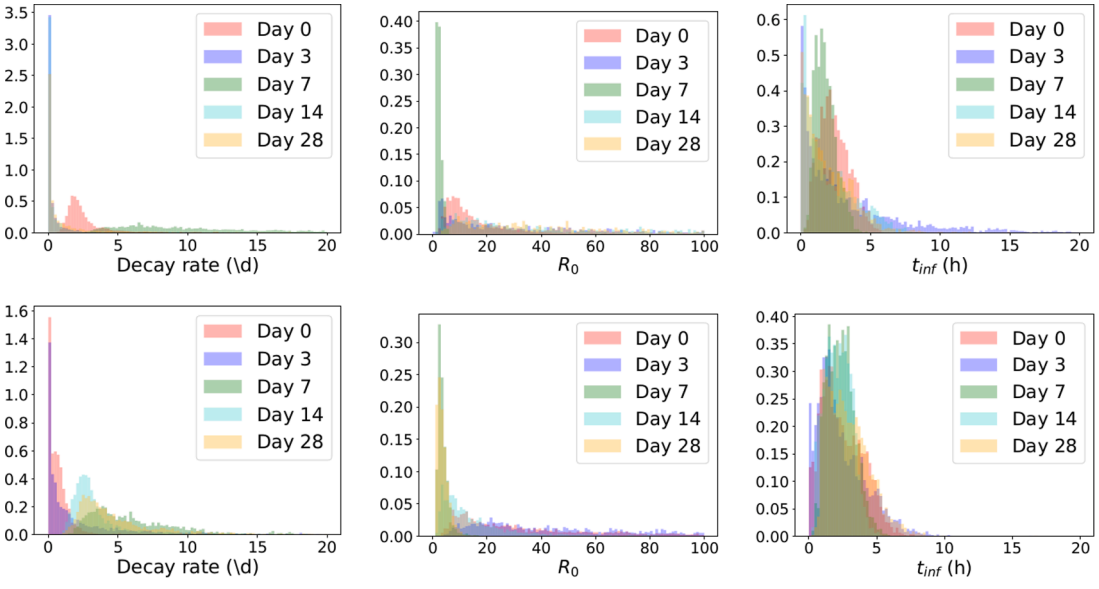

Fig. 4. Viral kinetics parameter estimates in different aged ferrets. We show the distributions of viral decay rate (left column), basic reproduction number (center column), and infecting time (right column) for RSV infections in ferret group 1 (top row) and ferret group 2 (bottom row).

immune response. A more detailed model that explicitly includes an immune response might capture parameter changes that are not apparent using a simplified model, as was done for influenza (Hernandez-Vargas et al., 2014; Keef et al., 2017). An extended model could also incorporate the effect of previous RSV exposure. Use of a more detailed model would require detailed time course measurements of any immune responses included in the model in order to properly identify additional model parameters (Miao et al., 2011). Explicit incorporation of immune responses in the model, along with experimental measurements of these responses, could also improve estimates of some of the basic viral kinetics parameters. For example, the parameter c currently represents an average viral clearance rate due to all possible viral clearance mechanisms. If the antibody response is explicitly represented in the model, and associated antibody time course measurements are used to help parameterize the antibody response, then c no longer includes the effect of viral clearance by antibodies, and the variance in estimates of c should decrease.

There are methodological issues with the experimental data here that might also be hindering our ability to detect any age-related trends. As noted in the methods, neither data set represents the viral time course of infection in a single animal. One study of influenza in patients found that using a single median viral titer curve does not result in the same parameter estimates as fitting individual patient curves (Hooker and Ganusov, 2021). The averaging of several measurements at each time point along with the fact that each measurement is from a different animal could render age-related changes in parameters undetectable. There is also noise in the experimental data (La Barre and Lowy, 2001), leading to uncertainty in the parameter estimates that could potentially mask any underlying age-related changes. Additionally, measurements are taken only daily and only viral load is measured. This results in not enough information to properly identify some of the model parameters. We note that our results have large 95% confidence intervals and broad posterior parameter distributions, which makes it difficult to identify small age-dependent effects like the change in onset of immune response found by Wethington et al. (2019). While it might be difficult to reduce experimental error, there are other tactics that could help make parameter estimates more precise (Nguyen et al., 2015; 2016; Petrie et al., 2013). A study examining the effect of sampling frequency on parameter estimation in an acute model of viral kinetics noted a continual diminishing of variance in the parameter estimates as sampling frequency increased to every 3 h (Nguyen et al., 2016). A study of parameter estimation in a viral kinetics model of chronic infection showed that the curvature of the cost function increases with increased sampling frequency, creating a sharper minimum and improving identifiability of the parameters (Portelo et al., 2013). Finally, another study showed that measurement of viral RNA, and inclusion of viral RNA in the model, improved the precision of parameter estimates (Petrie et al., 2013). In order to capture age-related trends, it is also necessary to include more animals of different ages. Unfortunately, many of these solutions require use of more animals or additional experimental techniques, which greatly increases the expense and time needed to conduct experiments.

The use of animal models could also lead to results that differ from RSV infections in humans (Altamirano-Lagos et al., 2019). A study of RSV viral kinetic infection parameters showed that the decay rate is higher in African Green monkeys than in humans, but that the infecting time is lower than in humans (González-Parra and Dobrovolny, 2018b), pointing to the possibility that parameter estimates in different animals might not correlate to human infections. The cotton rat model has the advantage that the innate immune response to RSV is similar to the innate immune response in humans (Boukhvalova and Blanco, 2013) and appears to provide similar maternal transfer of passive immunity (Blanco et al., 2015; Prince et al., 1983). However, there are drawbacks to this animal model. Spread of the infection to the trachea and lower respiratory tract does not mimic spread in the respiratory tracts of humans (Altamirano-Lagos et al., 2019; Boukhvalova and Blanco, 2013). There are also limited clinical manifestations and a lack of bronchiolitis (Prince et al., 1978), possibly indicating differences in the immune response to RSV infection. The ferret model is also thought to reproduce some aspects of changing RSV infections with age (Byrd and Prince, 1997). In particular, the decreasing penetration of virus into the lungs as young ferrets age (Prince and Porter, 1976) is similar to the trend observed in human infants. Unfortunately, there do not appear to be any studies yet examining early development of the immune response in young ferrets to assess whether the differences in infection dynamics are caused by changes in the immune response.

The lack of a clear trend in age-related changes to the parameters examined here highlights the need for further study of the development of the immune response to RSV. Experiments including more detailed measurements of viral time course and time course of immune responses as animals age will help tease out how viral dynamics change in response to a developing immune system.

CRediT authorship contribution statement

Shaheer Khan: Software, Validation, Formal analysis, Writing – original draft. **Hana M. Dobrovolny:** Conceptualization, Methodology, Validation, Formal analysis, Writing – review & editing, Supervision, Project administration.

Declaration of Competing Interest

The authors declare that they have no known competing financial interests or personal relationships that could have appeared to influence the work reported in this paper.

Supplementary material

Supplementary material associated with this article can be found, in the online version, at doi:10.1016/j.virusres.2021.198524.

References

Altamirano-Lagos, M.J., Diaz, F.E., Mansilla, M.A., Rivera-Perez, D., Soto, D., McGill, J. L., Vasquez, A.E., Kalergis, A.M., 2019. Current animal models for understanding the pathology caused by the respiratory syncytial virus. Front. Microbiol. 10, 873. https://doi.org/10.3389/fmicb.2019.00873.

Anderson, N.W., Binnicker, M.J., Harris, D.M., Chirila, R.M., Brumble, L., Mandrekar, J., Hata, D.J., 2016. Morbidity and mortality among patients with respiratory syncytial virus infection: a 2-year retrospective review. Diagn. Microbiol. Infect. Dis. 85 (3), 367–371. https://doi.org/10.1016/j.diagmicrobio.2016.02.025.

Baccam, P., Beauchemin, C., Macken, C.A., Hayden, F.G., Perelson, A.S., 2006. Kinetics of influenza A virus infection in humans. J. Virol. 80 (15), 7590–7599. https://doi.org/10.1128/JVI.01623-05.

Backman, K., Piippo-Savolainen, E., Ollikainen, H., Koskela, H., Korppi, M., 2014. Adults face increased asthma risk after infant RSV bronchiolitis and reduced respiratory health-related quality of life after RSV pneumonia. Acta Pediatrica 103 (8), 850–855. https://doi.org/10.1111/apa.12662.

Bagga, B., Woods, C.W., Veldman, T.H., Gilbert, A., Mann, A., Balaratnam, G., Lambkin-Williams, R., Oxford, J.S., McClain, M.T., Wilkinson, T., Nicholson, B.P., Ginsburg, G.S., DeVincenzo, J.P., 2013. Comparing influenza and RSV viral disease dynamics in experimentally infected adults predicts clinical effectiveness of RSV antivirals. Antivir. Ther. 18, 785–791. https://doi.org/10.3851/IMP2629.

Baraldi, E., Bonadies, L., Manzoni, P., 2020. Evidence on the link between respiratory syncytial virus infection in early life and chronic obstructive lung diseases. Amer. J. Perinatol. 37, S26–S30. https://doi.org/10.1055/s-0040-1714345.

Beauchemin, C.A., Kim, Y.-I., Yu, Q., Ciaramella, G., De Vincenzo, J.P., 2019. Uncovering critical properties of the human respiratory syncytial virus by combining in vitro assays and in silico analyses. PloS One 14 (4), e0214708. https://doi.org/10.1371/journal.pone.0214708.

Blanco, J.C., Pletneva, L.M., Oue, R.O., Patel, M.C., Boukhvalova, M.S., 2015. Maternal transfer of RSV immunity in cotton rats vaccinated during pregnancy. Vaccine 33 (41), 5371–5379. https://doi.org/10.1016/j.vaccine.2015.08.071.

Blunck, B.N., Aideyan, L., Ye, X., Avadhanula, V., Ferlic-Stark, L., Zechiedrich, L., Gilbert, B.E., Piedra, P.A., 2021. A prospective surveillance study on the kinetics of the humoral immune response to the respiratory syncytial virus fusion protein in adults in Houston, Texas. Vaccine 39 (8), 1248–1256. https://doi.org/10.1016/j.vaccine.2021.01.045.

Borchers, A.T., Chang, C., Gershwin, M.E., Gershwin, L.J., 2013. Respiratory syncytial virus — a comprehensive review. Clin. Rev. Allergy Immunol. 45 (3), 331–379. https://doi.org/10.1007/s12016-013-8368-9.

Boukhvalova, M.S., Blanco, J.C., 2013. The cotton rat Sigmodon Hispidus model of respiratory syncytial virus infection, vol. 372, pp. 347–358. https://doi.org/10.1007/978-3-642-38919-1_17.
Boukhvalova, M.S., Yim, K.C., Kuhn, K.H., Hemming, J.P., Prince, G.A., Porter, D.D., Blanco, J.C., 2007. Age-related differences in pulmonary cytokine response to respiratory syncytial virus infection: modulation by anti-inflammatory and antiviral treatment. J. Infect. Dis. 195 (4), 511–518. https://doi.org/10.1086/510628.
Brenes-Chacon, H., Garcia-Maurino, C., Moore-Clingenpeel, M., Mertz, S., Ye, F., Cohen, D.M., Ramilo, O., Mejias, A., 2021. Age-dependent interactions among clinical characteristics, viral loads and disease severity in young children with respiratory syncytial virus infection. Ped. Inf. Dis. J. 40 (2), 116–122. https://doi.org/10.1097/INF.0000000000002914.
Byrd, L.G., Prince, G.A., 1997. Animal models of respiratory syncytial virus infection. Clin. Infect. Dis. 25 (6), 1363–1368. https://doi.org/10.1086/516152.
Cao, P., Wang, Z., Yan, A.W., McVernon, J., Xu, J., Heffernan, J.M., Kedzierska, K., McCaw, J.M., 2016. On the role of CD8(+) T cells in determining recovery time from influenza virus infection. Front. Immunol. 7, 611. https://doi.org/10.3389/fimmu.2016.00611.
Chu, H.Y., Steinhoff, M.C., Magaret, A., Zaman, K., Roy, E., Langdon, G., Formica, M.A., Walsh, E.E., Englund, J.A., 2014. Respiratory syncytial virus transplacental antibody transfer and kinetics in mother-infant pairs in bangladesh. J. Infect. Dis. 210 (10), 1582–1589. https://doi.org/10.1093/infdis/jiu316.
Chung, H.L., Park, H.J., Kim, S.Y., Kim, S.G., 2007. Age-related difference in immune responses to respiratory syncytial virus infection in young children. Ped. Allergy Immunol. 18 (2), 94–99. https://doi.org/10.1111/j.1399-3038.2006.00501.x.
Coutts, J., Fullarton, J., Morris, C., Grubb, E., Buchan, S., Rodgers-Gray, B., Thwaites, R., 2020. Influenza virus-membrane fusion triggered by proton uncaging for single particle studies of fusion kinetics. Ped. Pulmonol. 55 (5), 1104–1110. https://doi.org/10.1002/ppul.24676.
Dobrovolny, H.M., Reddy, M.B., Kamal, M.A., Rayner, C.R., Beauchemin, C.A., 2013. Assessing mathematical models of influenza infections using features of the immune response. PLoS One 8 (2), e57088. https://doi.org/10.1371/journal.pone.0057088.
Drajac, C., Laubreton, D., Riffault, S., Descamps, D., 2017. Pulmonary susceptibility of neonates to respiratory syncytial virus infection: a problem of innate immunity? J. Immunol. Res. 8734504. https://doi.org/10.1155/2017/8734504.
Eichinger, K.M., Resetar, E., Orend, J., Anderson, K., Empey, K.M., 2017. Age predicts cytokine kinetics and innate immune cell activation following intranasal delivery of IFN gamma and GM-CSF in a mouse model of RSV infection. Cytokine 97, 25–37. https://doi.org/10.1016/j.cyto.2017.05.019.
Elahi, S., Ertelt, J.M., Kinder, J.M., Jiang, T.T., Zhang, X., Xin, L., Chaturvedi, V., Strong, B.S., Qualls, J.E., Steinbrecher, K.A., Kalfa, T.A., Shaaban, A.F., Way, S.S., 2013. Immunosuppressive CD71(+) erythroid cells compromise neonatal host defence against infection. Nature 504 (7478), 158–162. https://doi.org/10.1038/nature12675.
Fauroux, B., Simoes, E.A., Checchia, P.A., Paes, B., Figueras-Aloy, J., Manzoni, P., Bont, L., Carbonell-Estrany, X., 2017. The burden and long-term respiratory morbidity associated with respiratory syncytial virus infection in early childhood. Infect. Dis. Ther. 6 (2), 173–197. https://doi.org/10.1007/s40121-017-0151-4.
Garcia-Maurino, C.C., Moore-Clingenpeel, M., Thomas, J., Mertz, S., Cohen, D.M., Ramilo, O., Mejias, A., 2019. Viral load dynamics and clinical disease severity in infants with respiratory syncytial virus infection. J. Infect. Dis. 219 (8), 1207–1215. https://doi.org/10.1093/infdis/jiy655.
González-Parra, G., De Ridder, F., Huntjens, D., Roymans, D., Ispas, G., Dobrovolny, H. M., 2018. A comparison of RSV and influenza in vitro kinetic parameters reveals differences in infecting time. PloS One 13 (2), e0192645. https://doi.org/10.1371/journal.pone.0192645.
González-Parra, G., Dobrovolny, H.M., 2015. Assessing uncertainty in A2 respiratory syncytial virus viral dynamics. Comput. Math. Meth. Med. 2015, 567589. https://doi.org/10.1155/2015/567589.
González-Parra, G., Dobrovolny, H.M., 2018. Modeling of fusion inhibitor treatment of RSV in African green monkeys. J. Theor. Biol. 456, 62–73. https://doi.org/10.1016/j.jtbi.2018.07.029.
González-Parra, G., Dobrovolny, H.M., 2018. A quantitative assessment of dynamical differences of RSV infections in vitro and in vivo. Virol. 523, 129–139. https://doi.org/10.1016/j.virol.2018.07.027.
González-Parra, G., Dobrovolny, H.M., Aranda, D.F., Chen-Charpentier, B., Roja, R.A.G., 2018. Quantifying rotavirus kinetics in the REH tumor cell line using in vitro data. Virus Res. 244, 53–63. https://doi.org/10.1016/j.virusres.2017.09.023.
Hall, C., Long, C., Schnabel, K., 2001. Respiratory syncytial virus infections in previously healthy working adults. Clin. Inf. Dis. 33 (6), 792–796. https://doi.org/10.1086/322657.
Hernandez-Vargas, E.A., Velasco-Hernandez, J.X., 2020. In-host modelling of COVID-19 kinetics in humans. Annu. Rev. Control 50, 448–456. https://doi.org/10.1016/j.arcontrol.2020.09.006.
Hernandez-Vargas, E.A., Wilk, E., Canini, L., Toapanta, F.R., Binder, S.C., Uvarovskii, A., Ross, T.M., Guzman, C.A., Perelson, A.S., Meyer-Hermann, M., 2014. Effects of aging on influenza virus infection dynamics. J. Virol. 88 (8), 4123–4131. https://doi.org/10.1128/JVI.03644-13.
Hooker, K.L., Ganusov, V.V., 2021. Impact of oseltamivir treatment on influenza A and B virus dynamics in human volunteers. Front. Microbiol. 12, 631211. https://doi.org/10.3389/fmicb.2021.631211.
Kabego, L., Balol'Ebwami, S., Kasengi, J.B., Miyanga, S., Bahati, Y.L., Kambale, R., de Beer, C., 2018. Human respiratory syncytial virus: prevalence, viral co-infections and risk factors for lower respiratory tract infections in children under 5 years of age at a general hospital in the Democratic Republic of Congo. J. Med. Microbiol. 67 (4), 514–522. https://doi.org/10.1099/jmm.0.000713.
Keef, E., Zhang, L.A., Swigon, D., Urbano, A., Ermentrout, G.B., Matuszewski, M., Toapanta, F.R., Ross, T.M., Parker, R.S., Clermont, G., 2017. Discrete dynamical modeling of influenza virus infection suggests age-dependent differences in immunity. J. Virol. 91 (23), e00395-17. https://doi.org/10.1128/JVI.00395-17.
La Barre, D., Lowy, R., 2001. Improvements in methods for calculating virus titer estimates from $TCID_{50}$ and plaque assays. J. Virol. Meth. 96 (2), 107–126. https://doi.org/10.1016/S0166-0934(01)00316-0.
Lambert, L., Sagfors, A.M., Openshaw, P.J., Culley, F.J., 2014. Immunity to RSV in early-life. Front. Immunol. 5, 466. https://doi.org/10.3389/fimmu.2014.00466.
Lee, F.E.-H., Walsh, E.E., Falsey, A.R., Betts, R.F., Treanor, J.J., 2004. Experimental infection of humans with A2 respiratory syncytial virus. Antiviral Res. 63, 191–196. https://doi.org/10.1016/j.antiviral.2004.04.005.
Liao, L.E., Carruthers, J., Smither, S.J., Weller, S.A., Williamson, D., Laws, T.R., Garcia-Dorival, I., Hiscox, J., Holder, B.P., Beauchemin, C.A., Perelson, A.S., Lopez-Garcia, M., Lythe, G., Barr, J.N., Molina-Paris, C., 2020. Quantification of Ebola virus replication kinetics in vitro. PLoS Comput. Biol. 16 (11), e1008375. https://doi.org/10.1371/journal.pcbi.1008375.
Marr, N., Wang, T.-I., Kam, S.H., Hu, Y.S., Sharma, A.A., Lam, A., Markowski, J., Solimano, A., Lavoie, P.M., Turvey, S.E., 2014. Attenuation of respiratory syncytial virus-induced and RIG-I-dependent type I IFN responses in human neonates and very young children. J. Infect. Dis. 192 (3), 948–957. https://doi.org/10.4049/jimmunol.1302007.
Mcintosh, K., Masters, H., Orr, I., Chao, R., Barkin, R., 1978. Immunological response to infection with respiratory syncytial virus in infants. J. Infect. Dis. 138 (1), 24–32.
Miao, H., Xia, X., Perelson, A.S., Wu, H., 2011. On identifiability of nonlinear ODE models and applications in viral dynamics. SIAM Rev. 53 (1), 3–39. https://doi.org/10.1137/090757009.
Mills, J., Vankirk, J., Wright, P., Chanock, R., 1971. Experimental respiratory syncytial virus infection of adults — possible mechanisms of resistance to infection and illness. J. Immunol. 107 (1), 123–130.
Mold, J.E., Venkatasubrahmanyam, S., Burt, T.D., Michaelsson, J., Rivera, J.M., Galkina, S.A., Weinberg, K., Stoddart, C.A., McCune, J.M., 2010. Fetal and adult hematopoietic stem cells give rise to distinct T cell lineages in humans. Science 330 (6011), 1695–1699. https://doi.org/10.1126/science.1196509.
Nguyen, V.K., Binder, S.C., Boianelli, A., Meyer-Hermann, M., Hernandez-Vargas, E.A., 2015. Ebola virus infection modeling and identifiability problems. Front. Microbiol 6, 257. https://doi.org/10.3389/fmicb.2015.00257.
Nguyen, V.K., Klawonn, F., Mikolajczyk, R., Hernandez-Vargas, E.A., 2016. Analysis of practical identifiability of a viral infection model. PloS One 11 (12), e0167568. https://doi.org/10.1371/journal.pone.0167568.
Paradis, E.G., Pinilla, L.T., Holder, B.P., Abed, Y., Boivin, G., Beauchemin, C.A.A., 2015. Impact of the H275Y and I223V mutations in the neuraminidase of the 2009 pandemic influenza virus in vitro and evaluating experimental reproducibility. PloS One 10 (5), e0126115. https://doi.org/10.1371/journal.pone.0126115.
Petrie, S.M., Butler, J., Barr, I.G., McVernon, J., Hurt, A.C., McCaw, J.M., 2015. Quantifying relative within-host replication fitness in influenza virus competition experiments. J. Theor. Biol. 382, 259–271. https://doi.org/10.1016/j.jtbi.2015.07.003.
Petrie, S.M., Guarnaccia, T., Laurie, K.L., Hurt, A.C., McVernon, J., McCaw, J.M., 2013. Reducing uncertainty in within-host parameter estimates of influenza infection by measuring both infectious and total viral load. PloS One 8 (5), e64098. https://doi.org/10.1371/journal.pone.0064098.
Piedra, F.-A., Mei, M., Avadhanula, V., Mehta, R., Aideyan, L., Garofalo, R.P., Piedra, P. A., 2017. The interdependencies of viral load, the innate immune response, and clinical outcome in children presenting to the emergency department with respiratory syncytial virus-associated bronchiolitis. PloS One 12 (3), e0172953. https://doi.org/10.1371/journal.pone.0172953.
Pinilla, L.T., Holder, B.P., Abed, Y., Boivin, G., Beauchemin, C.A.A., 2012. The H275Y neuraminidase mutation of the pandemic A/H1N1 influenza virus lengthens the eclipse phase and reduces viral output of infected cells, potentially compromising fitness in ferrets. J. Virol. 86 (19), 10651–10660. https://doi.org/10.1128/JVI.07244-11.
Portelo, A., Lemos, J., Vinga, S., Ribeiro, R.M., Cruz, J., Valadas, E., 2013. Parameter estimation and identifiability of a HIV-1 model. 21st Mediterranean Conference on Control and Automation, pp. 691–696.
Prince, G.A., Horswood, R.L., Carmago, E., Koenig, D., Chanock, R.M., 1983. Mechanisms of immunity to respiratory syncytial virus in cotton rats. Infect. Immun. 42 (1), 81–87. https://doi.org/10.1128/IAI.42.1.81-87.1983.
Prince, G.A., Jenson, A.B., Horswood, R.L., Camargo, E., Chanock, R.M., 1978. The pathogenesis of respiratory syncytial virus infection in cotton rats. Am. J. Pathol. 93 (3), 771–791.
Prince, G.A., Porter, D.D., 1976. The pathogenesis of respiratory syncytial virus infection in infant ferrets. Am. J. Pathol 82 (2), 339–352.
Sande, C.J., Cane, P.A., Nokes, D., 2014. The association between age and the development of respiratory syncytial virus neutralising antibody responses following natural infection in infants. Vaccine 32 (37), 4726–4729. https://doi.org/10.1016/j.vaccine.2014.05.038.
Shi, T., Balsells, E., Wastnedge, E., Singleton, R., Rasmussen, Z., Zar, H.J., Rath, B.A., Madhi, S.A., Campbell, S., Vaccari, L.C., Bulkow, L.R., Thomas, E.D., Barnett, W., Hoppe, C., Campbell, H., Nair, H., 2015. Risk factors for respiratory syncytial virus associated with acute lower respiratory infection in children under five years: systematic review and meta-analysis. J. Global Health 5 (2), 203–215. https://doi.org/10.7189/jogh.05.020416.
Shrestha, B., You, D., Saravia, J., Siefker, D.T., Jaligama, S., Lee, G.I., Sallam, A.A., Harding, J.N., Cormier, S.A., 2017. IL-4R alpha on dendritic cells in neonates and

Th2 immunopathology in respiratory syncytial virus infection. J. Leukocyte Biol. 102 (1), 153–161. https://doi.org/10.1189/jlb.4A1216-536R.
Simon, P.F., de La Vega, M.A., Paradis, E., Mendoza, E., Coombs, K.M., Kobasa, D., Beauchemin, C.A.A., 2016. Avian influenza viruses that cause highly virulent infections in humans exhibit distinct replicative properties in contrast to human H1N1 viruses. Sci. Rep. 6, 24154. https://doi.org/10.1038/srep24154.
Smith, A.M., Adler, F.R., Perelson, A.S., 2010. An accurate two-phase approximate solution to an acute viral infection model. J. Math. Biol. 60 (5), 711–726. https://doi.org/10.1007/s00285-009-0281-8.
Stein, R.T., Bont, L.J., Zar, H., Polack, F.P., Park, C., Claxton, A., Borok, G., Butylkova, Y., Wegzyn, C., 2017. Respiratory syncytial virus hospitalization and mortality: Systematic review and meta-analysis. Pediatr. Pulmonol 52 (4), 556–569. https://doi.org/10.1002/ppul.23570.
Toivonen, L., Karppinen, S., Schuez-Havupalo, L., Teros-Jaakkola, T., Mertsola, J., Waris, M., Peltola, V., 2020. Respiratory syncytial virus infections in children 0–24 months of age in the community. J. Infect. 80 (1), 69–75. https://doi.org/10.1016/j.jinf.2019.09.002.
Trento, A., Rodriguez-Fernandez, R., Gonzalez-Sanchez, M.I., Gonzalez-Martinez, F., Mas, V., Vazquez, M., Palomo, C., Melero, J.A., 2017. The complexity of antibody responses elicited against the respiratory syncytial virus glycoproteins in hospitalized children younger than 2 years. Front. Microbiol. 8, 2301. https://doi.org/10.3389/fmicb.2017.02301.
Ueno, F., Tamaki, R., Saito, M., Okamoto, M., Saito-Obata, M., Kamigaki, T., Suzuki, A., Segubre-Mercado, E., Aloyon, H., Tallo, V., Lupisan, S.P., Oshitani, H., Landicho, J. M., Renosa, M.D.C., Inobaya, M.T., Alday, P.P., Tandoc, A., 2019. Age-specific incidence rates and risk factors for respiratory syncytial virus-associated lower respiratory tract illness in cohort children under 5 years old in the philippines. Influenza Other Resp. Viruses 13 (4), 339–353. https://doi.org/10.1111/irv.12639.
Uusitupa, E., Waris, M., Heikkinen, T., 2020. Association of viral load with disease severity in outpatient children with respiratory syncytial virus infection. J. Infect. Dis. 222 (2), 298–304. https://doi.org/10.1093/infdis/jiaa076.
Varga, S.M., Braciale, T.J., 2013. The adaptive immune response to respiratory syncytial virus. Challenges and Opportunities for Respiratory Syncytial Virus Vaccines, vol. 372, pp. 155–171. https://doi.org/10.1007/978-3-642-38919-1_8.
Vojvoda, V., Mlakar, A.S., Jergovic, M., Kukuruzovic, M., Markovinovic, L., Aberle, N., Rabatic, S., Bendelja, K., 2014. The increased type-1 and type-2 chemokine levels in children with acute RSV infection alter the development of adaptive immune responses. Biomed Res. Intl. 2014, 750521. https://doi.org/10.1155/2014/750521.
Walsh, E. E., Wang, L., Falsey, A. R., Qiu, X., Corbett, A., Holden-Wiltse, J., Mariani, T. J., Topham, D. J., Caserta, M. T., 2018. Virus-specific antibody, viral load and disease severity in respiratory syncytial virus infection. J. Infect. Dis. 218(2), 208–217. 10.1093/infdis/jiy106.
Wen, X., Mo, S., Chen, S., Yu, G., Gao, L., Chen, S., Deng, Y., Xie, X., Zang, N., Ren, L., Liu, E., 2019. Pathogenic difference of respiratory syncytial virus infection in cotton rats of different ages. Microb. Pathogen. 137, 103749. https://doi.org/10.1016/j.micpath.2019.103749.
Wethington, D., Harder, O., Uppulury, K., Stewart, W.C., Chen, P., King, T., Reynolds, S. D., Perelson, A.S., Peeples, M.E., Niewiesk, S., Das, J., 2019. Mathematical modelling identifies the role of adaptive immunity as a key controller of respiratory syncytial virus in cotton rats. J. Roy. Soc. Interface 16 (160), 20190389. https://doi.org/10.1098/rsif.2019.0389.
Zar, H.J., Nduru, P., Stadler, J.A., Gray, D., Barnett, W., Lesosky, M., Myer, L., Nicol, M. P., 2020. Early-life respiratory syncytial virus lower respiratory tract infection in a south african birth cohort: epidemiology and effect on lung health. Lancet Global Health 8 (10), E1316–E1325.
Zhou, L., Xiao, Q., Zhao, Y., Huang, A., Ren, L., Liu, E., 2015. The impact of viral dynamics on the clinical severity of infants with respiratory syncytial virus bronchiolitis. J. Med. Virol. 87 (8), 1276–1284. https://doi.org/10.1002/jmv.24111.